

Accounts

Excited-State Double-Proton Transfer in the 7-Azaindole Dimer in the Gas Phase. Resolution of the Stepwise versus Concerted Mechanism Controversy and a New Paradigm

Hiroshi Sekiya* **and Kenji Sakota**

Department of Chemistry, Faculty of Sciences, Kyushu University, 6-10-1 Hakozaki, Higashi-ku, Fukuoka 812-8581

Received August 30, 2005; E-mail: hsekiscc@mbox.nc.kyushu-u.ac.jp

The 7-azaindole dimer ($7AI_2$) is a prototype of double hydrogen-bonded molecules. $7AI_2$ has been considered as a model DNA base pair and has attracted much attention to the mechanism of the excited-state double-proton transfer (ESDPT). Two ESDPT mechanisms, stepwise and concerted mechanisms, have been proposed so far. Great efforts have been devoted to clarify the mechanism of ESDPT using experimental and theoretical methods. However, the reaction mechanism had been controversial for more than a decade. We provide the resolution of the two mechanisms on the basis of new data obtained from electronic spectroscopy and picosecond time-resolved spectroscopy in the gas phase. The initial state of the ESDPT reaction has been well characterized by investigating the exciton resonance interaction with UV–UV hole-burning spectroscopy for various $7AI_2$ isotopomers. The lowest-excited state of $7AI_2$ has been classified into the weak coupling case of the exciton theory. We have concluded that the ESDPT reaction in $7AI_2$ occurs via the concerted mechanism on the basis of the results of picosecond time-resolved experiments and the H/D kinetic isotope effect on ESDPT studied by measuring the vibronic-state selective dispersed fluorescence spectra. ESDPT of $7AI_2$ has a "*dynamic cooperative*" nature that may arise from the coupling of the two moving protons with the reorganization of electrons. We have provided a new paradigm of ESDPT, where two quantum effects, the exciton resonance interaction and the proton tunneling, are concerned with the ESDPT reaction.

Proton-transfer reactions are one of the most basic reactions, and they are important in physics, chemistry, and biology.[1–6] Spectroscopic studies on various proton-transfer systems combining with theoretical studies have provided rich information about the hydrogen-bonded structure and proton-transfer dynamics. In particular, a very detailed picture has been obtained for intramolecular single-proton transfer in polyatomic molecules, with laser spectroscopic measurements in the gas phase combining with theoretical studies. For example, a proton transfers by quantum mechanical tunneling mechanism when a potential energy barrier exists on a potential energy surface. The proton tunneling was clearly observed in the electronic and vibrational spectra of several polyatomic molecules.[6–10] Spectroscopic data and theoretical studies showed that the proton tunneling has a multi-dimensional nature, i.e., the motion of the moving proton couples with the coordinates of the heavy atoms that constitute the molecule. Such a multi-dimensional nature and quantum mechanical tunneling are important properties that characterize proton-transfer reactions. Now much effort is devoted to obtain a more complete picture for single-proton transfer reactions and also a new picture for more complicated multiproton-transfer reactions. There are many examples of multiproton-transfer reactions such as proton relay systems in enzymes, in hydrogen-bonded water complexes, and proton transfer in prototropic tautomerism. Multiproton-transfer reactions are of considerable interests in their hydrogen-bonded structures and dynamics.[11–15] In general, multiproton-transfer reaction dynamics is more complicated than the single-proton transfer dynamics, therefore, even for double-proton transfer, which is a prototype of multiproton-transfer, the mechanism has not been fully understood.

More than a half century ago the double-helix structure of DNA molecules was proposed by Watson and Crick. They pointed out that the rare tautomers of DNA bases might disturb the genetics code.[16] In 1963, Löwdin proposed the proton tunneling model of the origin of spontaneous point mutations in the DNA base pairs.[17] Since then, the proton-transfer reaction has been extensively investigated with model double hydrogen-bonded molecules. The 7-azaindole dimer ($7AI_2$) has been considered as a model DNA base pair, and it is one of the most widely studied double hydrogen-bonded dimers.[18–59] In the present paper, we focus on the excited-state double-proton transfer (ESDPT) in $7AI_2$. The observation of Stokes-shifted emission is a sign of the occurrence of ESDPT (Fig. 1).[18–20]

The time scale of ESDPT in $7AI_2$ ranges from subpicoseconds to picoseconds depending on the excitation energy of the UV light.[37,45] The appearance of strong fluorescence and a moderate time scale of the ESDPT reaction allow us to inves-

Published on the web March 8, 2006; DOI 10.1246/bcsj.79.373

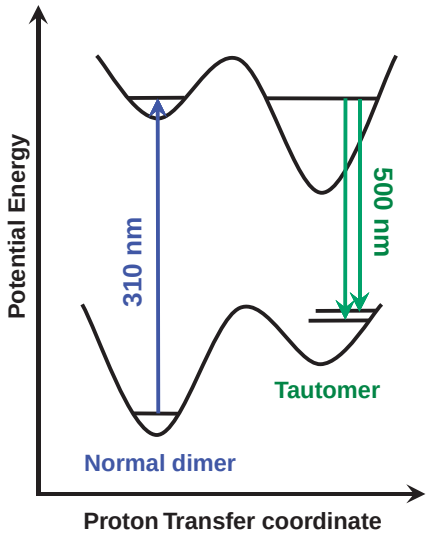

Fig. 1. Schematic drawing of one-dimensional potential energy curves for ESDPT reaction in $7AI_2$. The excitation of the normal dimer with UV light induces proton transfer to generate the excited state of the tautomer. The production of the tautomer is detected with visible light.

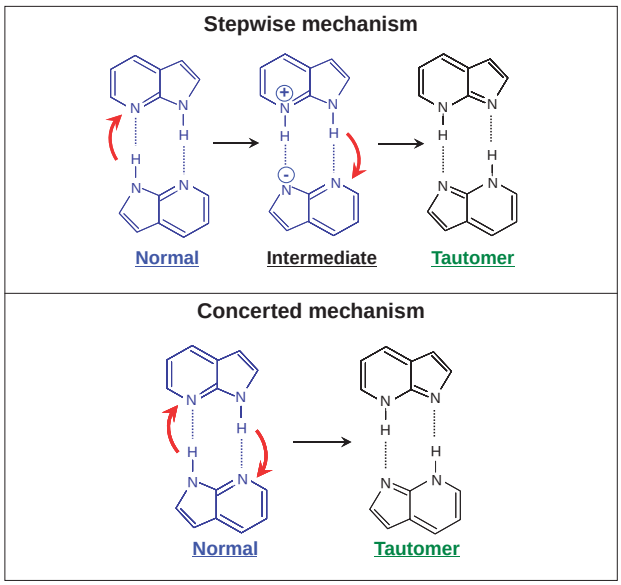

Fig. 2. Two mechanisms of ESDPT in $7AI_2$. The normal dimer undergoes single-proton transfer by photoexcitation to produce a stable zwitterionic state followed by second proton transfer to generate the tautomer. Two protons simultaneously transfer by photoexcitation of the normal dimer in the concerted mechanism, where no stable intermediate state exists.

tigate the ESDPT reaction dynamics in detail with laser spectroscopic methods. We consider that spectroscopic studies on $7AI_2$ provide basic information about the dynamics of multi-proton-transfer reactions involving quantum mechanical effects such as tunneling and interference in liquids and biological systems as well as in the gas phase.

Taylor, El-Bayoumi, and Kasha[18] were the first to observe the ESDPT reaction in $7AI_2$ by measuring the fluorescence spectrum in solution. Since then, numerous studies have focused on the mechanisms of ESDPT in $7AI_2$ in solution and matrix[19–34] and in the gas phase[35–47] by using various spectroscopic techniques. Theoretical studies have been also carried out to investigate the hydrogen-bonded structures, potential energy curves (or surface), and molecular dynamics of $7AI_2$.[48–58] Nevertheless, the ESDPT dynamics of $7AI_2$ has not been fully understood. Very recently, we extensively studied the ESDPT reaction in $7AI_2$ in the gas phase with frequency resolved and time-resolved spectroscopy.[42–45] In this paper, we provide final resolution of the stepwise versus concerted mechanism controversy regarding ESDPT in $7AI_2$. The discrepancies in the previous studies and important problems to be solved are summarized in Chaps. **1** and **2**. The experimental techniques used in our study are described in Chap. **3**. Our recent results and discussions are given in Chaps. **4**–**7**. We describe a new paradigm of ESDPT in $7AI_2$ in Chap. **8**. In Chap. **9**, we provide conclusions.

1. Stepwise and Concerted Mechanisms

Two mechanisms have been proposed for ESDPT in $7AI_2$ so far. Zewail and co-workers carried out the femtosecond time-resolved experiments by detecting the transient ions in a molecular beam.[37] They obtained decay profiles of the normal dimer (base pair) and its isotopomers by varying the excess energy in the S_1–S_0 region. Each decay profile was fitted to a bi-exponential function. For example, two time constants 650 fs and 3.3 ps were obtained when the excess energy is nearly zero. The short and long decay components were ascribed to a single-proton transfer from the normal dimer to a zwitterionic state and that from the intermediate state to the tautomer, respectively (Fig. 2).

Similar bi-exponential decay profiles were obtained for NH deuterated isotopomers. On the basis of the bi-exponential decays and the isotope effects, Zewail and co-workers proposed a "*stepwise mechanism*" (or sequential mechanism). After the report of Zewail's group,[37] Castleman's group introduced Coulomb explosion technique to arrest the intermediate state of $7AI_2$ (118 + 118 amu).[39–41] They observed a rise time (660 fs) and a decay time (5 ps) of an ion signal with 119 amu, which was ascribed to a counterpart of the single-proton transferred dimer generated by Coulomb explosion of the reaction intermediate dimer, while the other counterpart was assigned to the counterpart signal with 117 amu. These time constants were believed to agree well with the fast decay component (650 fs) and slow decay component (3.3 ps) of the femtosecond time-resolved study conducted by Zewail's group.[37]

The other mechanism of ESDPT is "*concerted mechanism*" (Fig. 2), which was proposed by Kasha and co-workers from a quantum mechanical intuition and steady-state electronic spectra in solution.[18,51–54] They consider that the excitation is delocalized on the two monomer units in the lowest excited state of $7AI_2$ due to a strong exciton resonance interaction. According to Kasha, Catalán, and co-workers[18,51–54] the geometry of $7AI_2$ in the lowest excited state is C_{2h} since the two monomer units are equivalent, therefore, the two protons should move simultaneously on a potential energy surface that has no potential minimum between the initially excited state and the lowest excited state of the tautomer.

The mechanism of ESDPT in $7AI_2$ in solution was extensively studied by two groups. Takeuchi and Tahara[30–32] carried out femtosecond fluorescence up-conversion measurement in solution. They examined the decay profiles by varying the excitation energy. When the pump laser provided excess energies each decay profile was fitted to a bi-exponential function, but a single exponential decay was observed when the red-edge of the S_1–S_0 absorption was excited. The single exponential decay was ascribed to the concerted mechanism. Zewail and co-workers[33,34] also investigated ESDPT in solution with femtosecond fluorescence up-conversion and the transient absorption measurements. They obtained similar time constants to those of Takeuchi and Tahara. The long decay component (1–1.1 ps) was assigned to ESDPT in the two studies. However, the interpretation of the short decay component is different between the two groups. The short time constant 200 fs was ascribed to the S_2–S_1 electronic relaxation by Takeuchi and Tahara,[30–32] but it was assigned by Fiebig et al.[34] to the single-proton transfer occurring within 250 fs from the normal dimer to an intermediate state.

The excited-state geometry and potential energy curve (or surface) along the reaction coordinate were calculated to explore the mechanism of ESDPT in $7AI_2$. The excitation is localized on one monomer unit in the optimized structure of the lowest excited state of $7AI_2$ by Douhal et al.[48–50] They obtained a potential minimum that corresponds to the reaction intermediate state. This result supported the stepwise mechanism. In contrast, there is no potential minimum in the intermediate on a potential energy curve by Catalán et al.[51,52] calculated on the assumption that the geometry in the lowest excited state belongs to the C_{2h} symmetry group. The calculated result by Catalán et al. supported the concerted mechanism. Catalán et al. also calculated the potential curves for the ionic state of $7AI_2$[53] to explain the result of Coulomb explosion.[39–41] The calculations showed that a single-proton transferred intermediate molecule (119 amu) is stable in the ionic state, because the potential barrier between the normal dimer ion and the intermediate ion is lower than that between the intermediate ionic state and the tautomer ionic state. Therefore, Catalán et al.[53,54] considered that single-proton transfer occurs in the ionic state and that the observation of the molecule (119 amu) by Coulomb explosion was not evidence of the stepwise mechanism.

2. Discrepancies in the Mechanism of ESDPT in $7AI_2$

We note the following discrepancies; (1) The width of the origin band in the fluorescence excitation spectrum reported by Fuke et al.[35,36] is 5 cm^{-1}, this value was revised to 2.7 cm^{-1} by our group.[44] The 2.7 cm^{-1} width corresponds to an ESDPT time of 2 ps, whereas the fast decay component measured by Douhal et al.[37] is much shorter (650 fs) than 2 ps. (2) Kasha and co-workers[18,51–54] considered that the excitation is delocalized in the lowest excited state, whereas that is completely localized in the structure calculated by Douhal et al.[48–50] That is, the structure of the initial state of ESDPT is very different for each of the two groups. The determination of the stepwise versus concerted mechanism should be provided on the basis of clear data obtained from the gas-phase experiment. Femtosecond spectroscopy is a powerful tool to investigate the excited-state dynamics. However, this spectroscopy cannot selectively excite the single vibronic state. In the case of $7AI_2$, we should realize that the ESDPT rate substantially depends on the excited vibronic state. This specific nature was not taken into account to analyze the data obtained by the femtosecond experiments. It is crucial to use the picosecond pulse in order to excite single vibronic state and to examine the validity of the stepwise mechanism.[45]

We note that two quantum mechanical effects, exciton resonance interaction and proton tunneling, are involved in the ESDPT reaction. The exciton resonance interaction has been extensively investigated for the normal $7AI_2$ dimer (base pair) and its isotopomers.[43] The dispersed fluorescence spectrum of $7AI_2$ in the gas phase was observed only for the undeuterated dimer, but there has been no report for the isotopomers. The H/D kinetic isotope effects (KIE) on the ESDPT reaction has been studied by Douhal et al.[37] by time-resolved femtosecond spectroscopy. However, the KIE should be reinvestigated because the vibrational-mode dependent ESDPT was not taken into account for the interpretation of the decay profiles.[44]

3. Experimental Methods

Some experiments in both the time-domain and the frequency-domain have been used to investigate the excited-state dynamics of $7AI_2$ in the gas phase.[42–45] The experimental apparatus for the fluorescence excitation (FE) and the dispersed fluorescence (DF) spectroscopy, UV–UV hole-burning spectroscopy at Kyushu University is described in detail elsewhere.[42–44,60–62] Figure 3 displays the principle of the hole-burning spectroscopy to separate the vibronic transitions of isotopomers of $7AI_2$. The fluorescence from a specific vibronic state excited by a probe pulse is monitored, while the pump laser pulse excites the molecule prior to the probe pulse. A typical delay time for the two laser pulses is 800 ns. When the energy of the pump laser is nonresonant with the vibronic transition of the probed molecule, the intensity of fluorescence does not change, but when it is resonant with the transitions of the probed molecule a fluorescence dip appears. By tuning the wavenumber of the pump laser one can obtain the hole-

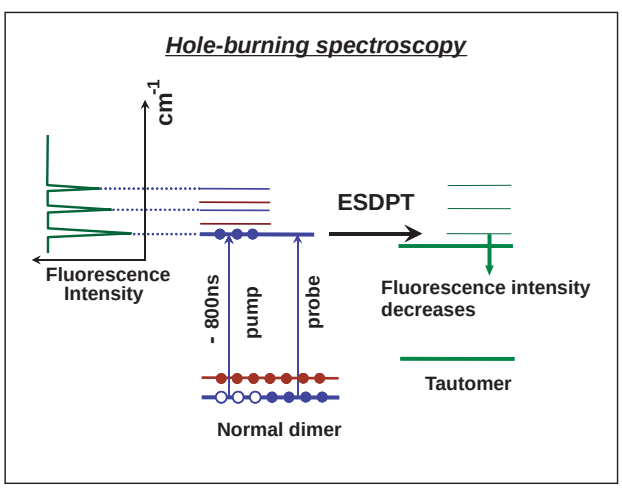

Fig. 3. UV–UV hole-burning spectroscopy for separations of the transitions of $7AI_2$ isotopomers. The principle of this spectroscopy is described in the text.

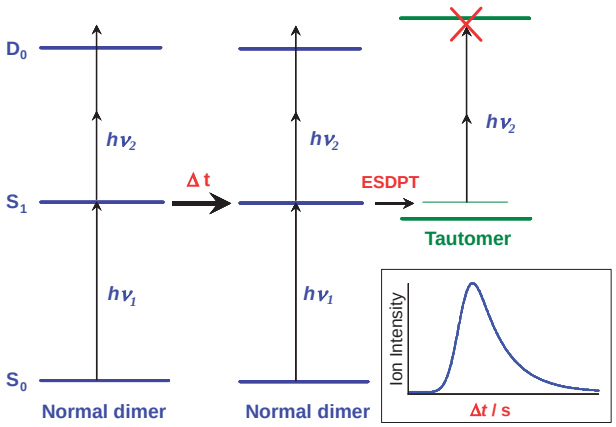

Fig. 4. The principle of time-resolved pump–probe spectroscopy is illustrated. The decay profiles of the normal dimer of $7AI_2$ are measured with the REMPI method (see the text). D_0 is the electronic ground state of the cationic dimer, while Δt is the delay time between the pump and probe lasers.

burning spectrum. The UV–UV hole-burning spectroscopy allows us to separate vibronic transitions of the deuterated $7AI_2$ dimers from those of the undeuterated dimer and plays a key role to characterize the excited vibronic state of $7AI_2$. The UV–UV hole-burning spectra were measured by using a frequency-doubled dye-laser (Spectra Physics PDL-3 and Inrad Autotracker III) pumped by a second harmonic of the Nd^{3+}:YAG laser (Spectra Physics GCR 18) as a pump laser.

Picosecond time resolved measurements were carried out at the Institute for Molecular Science. Our experimental system for picosecond time-resolved study is described in several references.[45,63,64] Figure 4 displays the principle of picosecond time-resolved resonance-enhanced multiphoton ionization (REMPI) spectroscopy to measure the decays of the excited normal $7AI_2$ dimer. The pump laser excites $7AI_2$ in a specific single vibronic state of the normal dimer, subsequently the probe laser ionizes the normal dimer. The energy of the probe laser is insufficient to ionize the tautomer, therefore, only the excited state of the normal dimer undergoes ionization by the probe laser. Thus, the decay profiles of the excited vibronic states are obtained by changing the delay time between the pump and probe lasers and then detecting the dimer ion signals that are mass-selected with a time-of-flight (TOF) mass spectrometer.

4. Reactive and Non-Reactive Dimers

Fuke et al.[35,36] observed the electronic spectrum of $7AI_2$ in a supersonic free jet expansion. They observed two transition systems, whose origins are identified at 32252 and 32290 cm^{-1}, respectively. Two progressions due to the intermolecular stretching mode (σ), the intermolecular bending mode (β), and the combination bands of σ and β were observed in a system that has an origin at 32252 cm^{-1}. A prominent finding is that the bandwidth of a vibronic band remarkably depends on the vibrational mode.[35,36] The deuteration of the NH hydrogen atom(s) decreases the bandwidth, indicating that ESDPT occurs in $7AI_2$ and deuterated dimers by a tunneling mechanism.

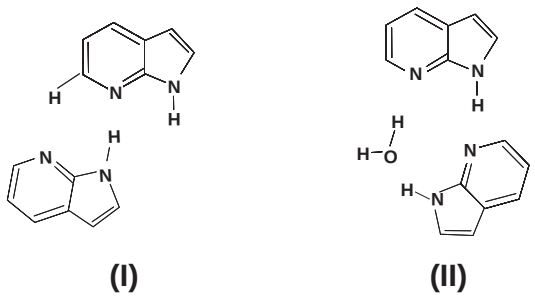

Fig. 5. Structures of non-reactive dimers proposed by Catalán et al. (I) and Yokoyama et al. (II). These structures are depicted based on Refs. 53 and 47.

A vibronic band at 32290 cm^{-1} in the fluorescence excitation spectrum of $7AI_2$ was assigned to the electronic origin of a non-reactive dimer.[35,36] A high-resolution spectrum of the non-reactive dimer by Nakajima et al.[46] suggested that the non-reactive dimer has a T-shaped structure. Catalán et al.[53] predicted a planar non-reactive $7AI_2$ dimer, as illustrated in Fig. 5(I). Recently, Fujii and co-workers[47] measured the infrared spectrum of the non-reactive dimer in the gas phase. They noted that a signal due to a free OH stretching vibration of water was observed at 3706 cm^{-1}. By combining the experimental IR spectrum with theoretical one, Fujii and co-workers concluded that a water molecule is hydrogen bonded between the two 7-azaindole moieties,[47] as illustrated in Fig. 5(II). The difficulty in the identification of this dimer originated from the loss of the water molecule upon photoionization.[35,41]

5. Nature of the Lowest Excited State of $7AI_2$

5.1 UV–UV Hole-Burning Spectra of $7AI_2$-*hd* and $7AI_2$-*dd*. The FE spectrum of the deuterated $7AI_2$ dimers in a supersonic free jet expansion was measured by Fuke et al.[36] However, the assignment of vibronic bands was not confirmed by using either mass-selected REMPI spectroscopy or UV–UV hole-burning spectroscopy. The analysis of the electronic spectra of the deuterated $7AI_2$ is important to investigate the mechanism of the ESDPT reaction, because ESDPT in $7AI_2$ occurs via proton tunneling.

Figure 6a shows the FE spectrum of a mixture of undeuterated and deuterated $7AI_2$.[42] The introduction of D_2O generates hydrogen-bonded complexes of $7AI_2$ with D_2O. Fluorescence from the hydrogen-bonded $7AI_2$–D_2O complexes was eliminated by using a cut-off filter to detect only the red-shifted tautomer fluorescence originating from the reactive $7AI_2$ dimer. In Fig. 6a, the vibronic bands of the deuterated dimers are superimposed on the vibronic bands of undeuterated $(7AI)_2$-*hh* in the FE spectrum. In order to separate the vibronic bands of isotopomers, the UV–UV hole-burning spectra are measured by probing the bands at 32293 and 32472 cm^{-1}. Figure 7 shows an enlarged part of the hole-burning spectrum in Fig. 6b. The band at 32293 cm^{-1} in Fig. 7 is assigned to an origin of $7AI_2$-*hd*, where one of the NH protons is deuterated. Another origin is identified at 21 cm^{-1} above the origin at 32293 cm^{-1}. Thus, two vibronic transition systems that have origins denoted by label **A** and **B** are overlapping in the UV–UV hole-burning spectrum of $7AI_2$-*hd* in Fig. 7. The nature of the lowest excited state of $7AI_2$-*hd* is discussed in more detail in Chaps. **5.3**

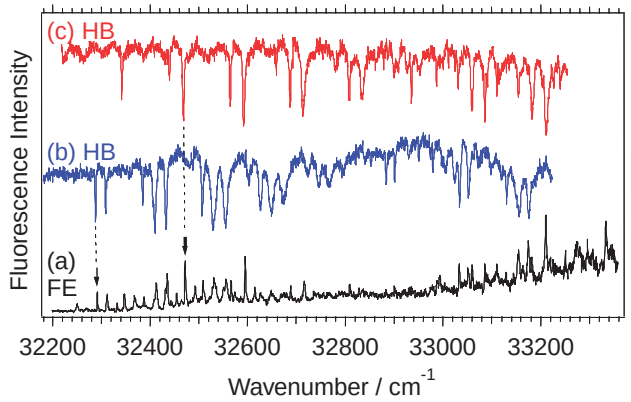

Fig. 6. Fluorescence excitation spectrum of a mixture of 7AI$_2$-*hh* and deuterated dimers in a supersonic free jet expansion obtained by monitoring visible emission (a). UV–UV hole-burning spectra measured by probing the vibronic band at 32293 cm^{-1} (b) and the band at 32472 cm^{-1} (c). The positions of these bands are indicated with the arrows in Fig. 6a. This figure was made based on Ref. 42.

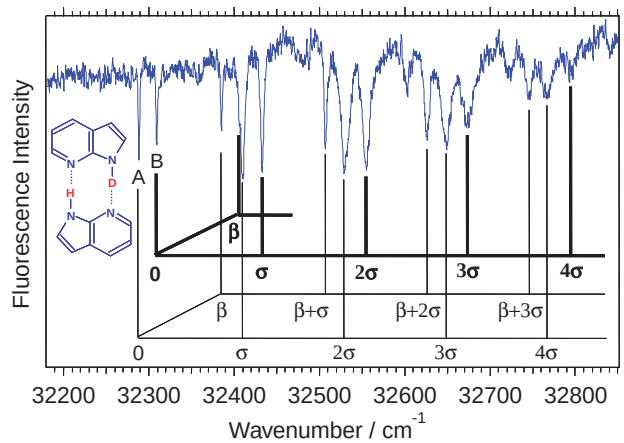

Fig. 7. Hole-burning spectrum of a deuterated 7AI$_2$ obtained by probing the vibronic band at 32293 cm^{-1}. Two systems are assigned to 7AI$_2$-h^*d and 7AI$_2$-hd^*, where the excitation is localized on one monomer unit 7AI-h^* and 7AI-d^*, respectively. **A** and **B** are origins of 7AI$_2$-h^*d and 7AI$_2$-hd^* (see the text). This figure was made based on Ref. 42.

and **5.4**. The hole-burning spectrum in Fig. 6c is assigned to 7AI$_2$-*dd*, where two NH protons are deuterated, because the vibronic structure is similar to 7AI$_2$-*hh* and the bandwidths are much narrower than the corresponding vibronic bands of 7AI$_2$-*hd*. The wavenumbers, assignments, and the bandwidths are summarized in Table 1.

5.2 Which States Will Be Excited with a Femtosecond Laser? The hole-burning spectrum of 7AI$_2$-*dd* is shown in Fig. 8 together with the FE spectrum of 7AI$_2$-*hh*. It should be noted that the vibronic bands due to the stretching (σ) and bending (β) modes are closely located. In Fig. 8, we draw a profile of a Gaussian function that was predicted from the reported width of the femtosecond laser (≈150 fs) and the excess energy ($\Delta E = 1.0$ kcal).[37] One can infer that more than two vibronic bands with longer and shorter lifetimes will be excited

Table 1. Fluorescence Excitation Spectra of 7AI$_2$-*dd*, 7AI$_2$-*hd*, and 7AI$_2$-*hh* and Assignment for Intermolecuar Vibrations[a)]

Species	$\Delta\nu$/cm^{-1} [c)]	Bandwidth/cm^{-1}	Assignment[e)]
7AI$_2$-*dd*	0 (32348)	—[d)]	Origin
	98	—[d)]	β
	124	2.6	σ
	222	1.7	$\beta+\sigma$
	247	2.6	2σ
	344	1.7	$\beta+2\sigma$
	368	5.1	3σ
	465	2.6	$\beta+3\sigma$
	487	5.1	4σ
7AI$_2$-h^*d	0 (32293)	1.6	Origin
	96	1.7	β
	121	4.1	σ
	216	2.8	$\beta+\sigma$
	239	—[d)]	2σ
7AI$_2$-hd^*	0 (32314)	1.6	Origin
	96	—[d)]	β
	123	2.4	σ
	243	5.2	2σ
7AI$_2$-*hh*	0 (32252)	2.7	Origin
	98	2.7	β
	120	10	σ
	215	7[b)]	$\beta+\sigma$
	240	3[b)]	2σ

a) Ref. 42. b) Ref. 35. c) Relative wavenumber from the electronic origin. The number in the parentheses indicates the wavenumber of the electronic origin. d) Bandwidth was not determined due to overlapping of bands. e) β and σ denote the intermolecular bending and stretching vibrations, respectively.

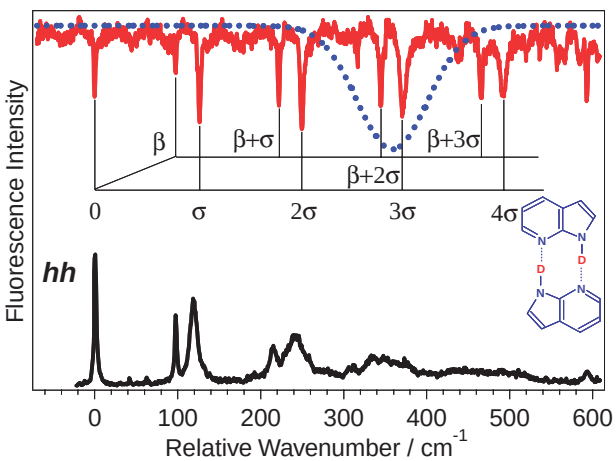

Fig. 8. The FE spectrum of undeuterated 7AI$_2$-*hh* (lower) and the hole-burning spectrum of 7AI$_2$-*dd*. The dotted line is a predicted profile of femtosecond laser (fwhm ≈150 fs and $\Delta E = 1.0$ kcal (Ref. 37), where a Gaussian function is assumed. This figure was made based on Ref. 42.

with the ≈150 fs pulse. Thus, femtosecond laser pulse could not separately excite the single vibronic state. This must be the origin of the bi-exponential decays observed by Zewail and

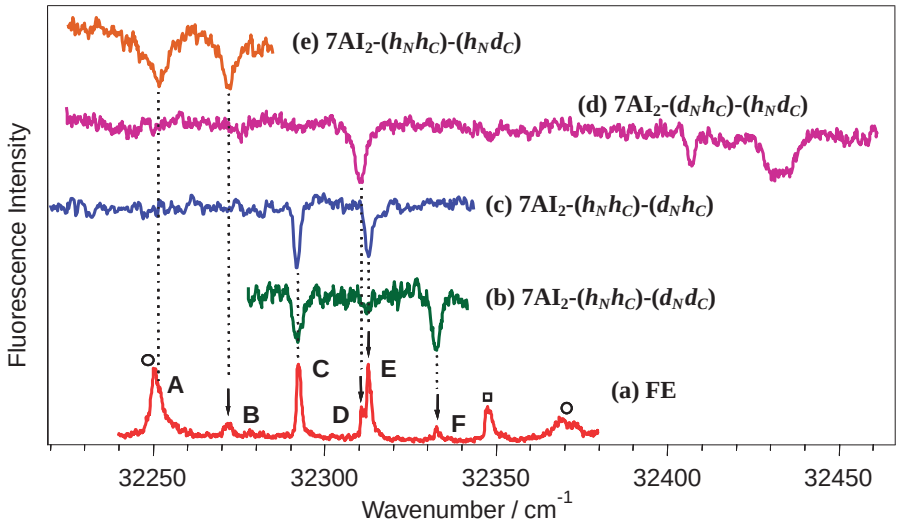

Fig. 9. FE spectrum of the undeuterated and deuterated $7AI_2$ obtained by monitoring the visible emission (a) and the UV–UV hole-burning spectra obtained by probing fluorescence from bands (b) **F**, (c) **E**, (d) **D**, and (e) **B**, respectively. The bands due to $7AI_2$-(h_Nh_C)-(h_Nh_C) and $7AI_2$-(d_Nh_C)-(d_Nh_C) are marked with the open circles and the open square, respectively. This figure was made based on Ref. 43.

co-workers.[37] We have confirmed this idea by the picosecond time-resolved study[45] described in Chap. **6**.

5.3 UV–UV Hole-Burning Spectra of Various Isotopomers. The concerted mechanism proposed by Kasha's group[18,51–54] is based on the strong coupling case of the exciton theory.[65–70] In contrast, theoretical calculations by Douhal et al.[48–50] showed that the excitation is completely localized on one monomer unit in the lowest excited state of $7AI_2$. On the other hand, Kanamaru[70] proposed that the lowest-excited state of $7AI_2$ should be classified into the weak coupling case on the basis of similar vibronic patterns in the one-photon and two-photon excitation spectra in the gas phase measured by Fuke et al.,[35,36] although they assigned the electronic spectra as the strong coupling case. Clear experimental data are necessary to understand the exciton resonance interaction in $7AI_2$.

Figure 9a shows the FE spectrum of a mixture of undeuterated and deuterated $7AI_2$ near the 0–0 region of the transition from the electronic ground state to the lowest-excited electronic state. The bands due to the introduction of D_2O are denoted by labels **A**–**F**. The intensities of bands **B**, **D**, and **F** are smaller than those of bands **C** and **E**. Bands **B**, **D**, and **F** appeared two days after the introduction of D_2O in the nozzle housing, whereas **C** and **E** appeared after one hour. The deuteration may more easily occur in the N–H bond than in the C–H bonds owing to a larger pK_a value for the N–H bond. Therefore, bands **A**, **B**, **D**, and **F** arise from the dimers having a C–D bond, while only N–H was deuterated in **C** and **E**. It is known that the C–D deuteration preferentially occurs at the 3-position. Bands **A**–**F** observed in the FE and hole-burning spectra are correlated to the excited-state structures of isotopomers in Fig. 10, where each of three pairs: (**A**, **B**), (**C**, **E**), and (**C**, **F**), is connected by the arrows. The wavenumbers and assignments are summarized in Table 2.

A prominent finding is that the two vibronic transitions to $7AI_2$-$(h_Nh_C)^*$-(d_Nh_C) (7AI-*hd* in Chap. **5.1**) and $7AI_2$-$(h_Nh_C)^*$-(d_Nd_C) are overlapping as band **C** observed in the FE spectrum since 7AI-(h_Nh_C) exists as a common monomer unit in $7AI_2$-$(h_Nh_C)^*$-(d_Nh_C) and $7AI_2$-$(h_Nh_C)^*$-(d_Nd_C), which are referred to as $\mathbf{C_{C-H}}$ and $\mathbf{C_{C-D}}$, respectively, in Fig. 10. However, the corresponding pairs **E** and **F** are observed at higher wavenumbers and the positions are different.

The zero-point energies change due to the deuteration of NH and/or CH. If the exciton resonance interaction occurs in the excited state its strength must be different for each of the two dimers $7AI_2$-(h_Nh_C)-(d_Nh_C) and $7AI_2$-(h_Nh_C)-(d_Nd_C), and the transition energies should be different. However, the overlapping of bands $\mathbf{C_{C-H}}$ [$7AI_2$-$(h_Nh_C)^*$-(d_Nh_C)] and $\mathbf{C_{C-D}}$ [$7AI_2$-$(h_Nh_C)^*$-(d_Nd_C)] indicates that the excitation is completely localized. Similarly, the excitation is completely localized in **A** and **B**.

The dimer which provides band **D** has a common monomer that has a unit with N–D as the dimer giving band **E**. If band **D** is due to a localized state, the position of band **D** should be the same as band **E**. However, band **D** is shifted by $2.1 \pm 1.0\,cm^{-1}$ from band **E**. Thus, band **D** has been assigned to [$7AI_2$-(d_Nh_C)-$(h_Nd_C)]^*$, where the zero-point levels of the two monomer units are nearly degenerated and the exciton resonance occurs. The electronic transition from the S_0 state to the higher wavenumber component of exciton splitting is forbidden; therefore, only the transition to the lower wavenumber component may appear as band **D**.

5.4 Strong Coupling Case or Weak Coupling Case. The exciton-resonance interaction is classified into two cases. One is the strong coupling case and the other is the weak coupling case. In the strong coupling case where the resonance integral is large, the ground-state and excited-state vibronic wave functions, $\Psi_{G,vw}$ and $\Psi_{\pm,vw}$, are expressed as[18,66–70]

$$\Psi_{G,vw} = \phi_a\phi_b\chi_v(Q_a)\chi_w(Q_b), \quad (1)$$

$$\Psi_{\pm,vw} = \frac{1}{\sqrt{2}}[\phi'_a\phi_b \pm \phi_a\phi'_b]\chi'_v(Q_a)\chi'_w(Q_b), \quad (2)$$

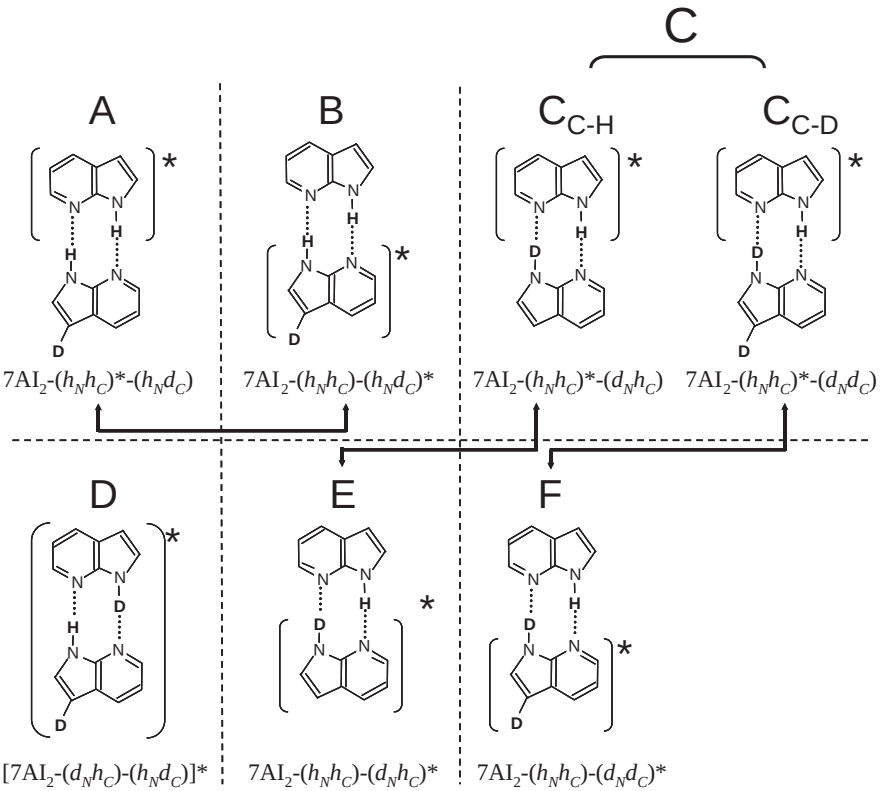

Fig. 10. The vibronic bands (**A**–**F**) in Fig. 10 are correlated to the excited-state structures. The asterisks indicate the electronically excited monomer units. Two structures (**A**, **B**), (**C**, **E**), and (**C**, **F**) linked by the arrows have a common structure in the electronic ground state. Only one structure exists for the excited state of **D**. Two dimers 7AI$_2$-($h_N h_C$)*-($d_N h_C$) and 7AI$_2$-($h_N h_C$)*-($d_N d_C$) provide band **C** in the FE spectrum. The structures of the two dimers are discriminated with notations $\mathbf{C}_{C-H}$ and $\mathbf{C}_{C-D}$. This figure was cited from Ref. 43.

Table 2. Wavenumbers of the 0–0 Transitions of 7AI$_2$ Isotopomers in the FE Spectrum[a)]

Bands	$\tilde{\nu}$/cm^{-1}	Isotopomer[b)]
A	32252	7AI$_2$-($h_N h_C$)*-($h_N d_C$)
B	32273	7AI$_2$-($h_N h_C$)-($h_N d_C$)*
$\mathbf{C}_{C-H}$	32293	7AI$_2$-($h_N h_C$)*-($d_N h_C$)
$\mathbf{C}_{C-D}$	32293	7AI$_2$-($h_N h_C$)*-($d_N d_C$)
D	32311	[7AI$_2$-($d_N h_C$)-($h_N d_C$)]*
E	32314	7AI$_2$-($h_N h_C$)-($d_N h_C$)*
F	32334	7AI$_2$-($h_N h_C$)-($d_N d_C$)*

a) Ref. 43. The 0–0 band of undeuterated 7AI$_2$ is observed at 32251 cm^{-1}. b) The asterisks indicate the electronically excited units in the dimer.

where ϕ_i and ϕ_i' are the ground-state and excited-state electronic wave functions of the two monomers, respectively, and $\chi_v(Q_i)$ and $\chi_w'(Q_i)$ are the ground-state and excited-state vibrational wave functions with the vibrational quantum number v and w, respectively, while subscripts a and b distinguish between the two monomer units. Equation 2 indicates that the *electronic wave functions* are delocalized over the dimer due to the exciton resonance interaction, and the vibrational wave functions in the excited states are described on new excitonic potential energy surfaces.

In the weak coupling case,[66–70] the excited-state vibronic wave functions $\Psi_{\pm,vw}$ are expressed as

$$\Psi_{\pm,vw} = C_1\phi_a'\phi_b\chi_v'(Q_a)\chi_w(Q_b) \pm C_2\phi_a\phi_b'\chi_w(Q_a)\chi_v'(Q_b). \quad (3)$$

When complete resonance occurs, $C_1 = C_2 = 1/\sqrt{2}$, while $C_1 \approx 1$ and $C_2 \approx 0$, or $C_1 \approx 0$ and $C_2 \approx 1$ for the completely localized case. Equation 3 indicates that the excitonic vibronic states should be described by the exciton interaction between the localized vibronic states in the weak coupling case.

In Chap. **5.3**, we described about the observation of the locally excited states in the asymmetrically deuterated 7AI$_2$ dimers, i.e. (**A**, **B**), ($\mathbf{C}_{C-H}$, **E**), and ($\mathbf{C}_{C-D}$, **F**) in Figs. 9 and 10. In the strong coupling case, the locally excited states cannot be observed due to the asymmetrical deuteration because the potential energy surface does not change by the deuteration and the excitonic states must be conserved even in the asymmetrically deuterated 7AI$_2$ dimers. Therefore, the electronic spectra of 7AI$_2$ isotopomers analyzed in Chap. **5.3** indicate that the lowest-excited electronic state (S_1) of 7AI$_2$ should be treated by the weak coupling case of the exciton theory. The potential curve along the coordinate where the exciton interaction occurs has a double well, in which exciton transfer occurs between the two wells by tunneling and the vibronic states in the potential well split into doublets. If the difference of the zero point energy in the left-hand side and the right-hand side potential well is larger than the interaction strength, the excitation easily localizes on the single potential well. This is the situation of the asymmetrically deuterated 7AI$_2$ dimers. Our recent studies on the (3-methyl-7-azaindole)$_2$ dimer[71] and

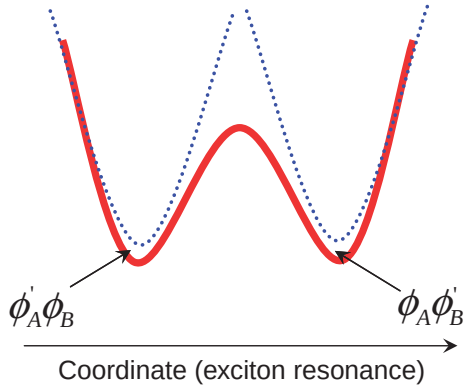

Fig. 11. A double-minimum potential for the weak coupling case. Two single-minimum potential curves for zeroth order locally excited states are indicated with broken lines.

the (3-methyl-7-azaindole)-(7-azaindole) heterodimer[72] showed that ESDPT rate does not significantly change due to the substitution of a methyl group. This suggests that the shape of the ESDPT potential of the (3-methyl-7-azaindole)-(7-azaindole) heterodimer is similar to that of the homodimers $7AI_2$ and (3-methyl-7-azaindole)$_2$. It should be noted that the exciton resonance interaction disappears in the heterodimer because the transition energies of the two locally excited states, (3-methyl-7-azaindole)*-(7-azaindole) and (3-methyl-7-azaindole)-(7-azaindole)*, are very different. Therefore, ESDPT in the heterodimer occurs from the locally excited state. These results are consistent with the weak coupling case, because the potential surfaces of the homodimers have strong nature of the locally excited state in the weak coupling case, as illustrated in Fig. 11.

Recently, the exciton resonance interaction has been studied for similar double hydrogen-bonded dimers, such as pyridone dimer[73–75] and anthralinic acid dimer[76] in the gas phase. The exciton resonance interaction strongly depends on the distance between the two monomer moieties as well as on the magnitude of the transition dipole moment. In the case of double hydrogen-bonded dimers, the distance between the two monomer units is restricted by the hydrogen-bond distances, therefore, in general the exciton interaction may be weak as compared with the aromatic dimers without intermolecular hydrogen bonds. To the best of our knowledge, the $7AI_2$ dimer is the first molecule whose excited state is clearly classified into the weak coupling case of the exciton theory.

6. Picosecond Time-Resolved Study

The photoelectron spectrum of $7AI_2$ was measured by Lopez-Martens et al.[38] with picosecond and subpicosecond lasers. By comparing the intensities between the two photoelectron spectra, Lopez-Martens et al. estimated the ESDPT time constant to be faster than a few picoseconds. Femtosecond time-resolved studies were carried out by Douhal et al.[37] and Folmer et al.[39–41] in the gas phase. As stated in the introduction the two groups concluded that the ESDPT reaction proceeds via the stepwise mechanism. However, the FE spectrum of $7AI_2$ exhibits closely spaced vibronic bands. In order to selectively excite a single vibronic state and determine the ESDPT rate constant, one must use the picosecond laser pulse which has enough energy resolution.

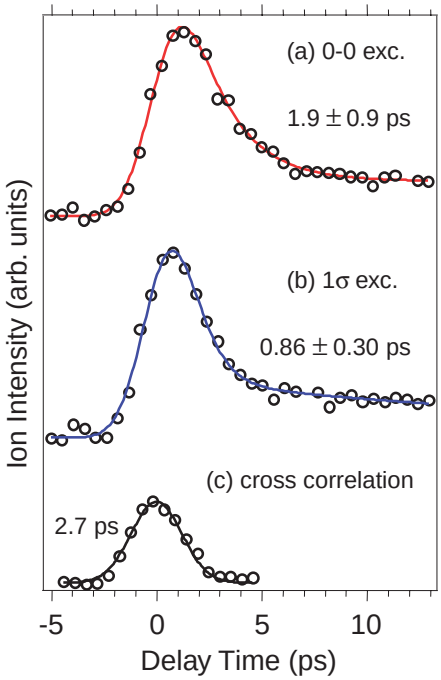

Fig. 12. Decay profiles of $7AI_2$-*hh* pumped at (a) the origin and (b) the intermolecular stretching band, respectively. The wavelength of the probe laser was fixed at 620 nm in (a) and (b). The open circles are experimental data, while the solid curves are best-fitted curves obtained by bi-exponential functions. The cross correlation trace is also indicated in (c). The instrumental time resolution given by the fwhm of the cross-correlation trace is 2.7 ps. This figure was made based on Ref. 45.

Figures 12a and 12b show the time profiles of the ion signal intensities of $7AI_2$ following the excitation of the origin and the intermolecular stretch fundamental (1σ), respectively. The time profiles in Figs. 12a and 12b are well reproduced by the convolutions of the response functions shown in Fig. 12c with bi-exponential decay profiles having the short and long time constants, respectively. In both profiles, the components of the time profiles with long lifetimes (>250 ps) are observed. The intensities of the decay components with the long lifetimes strongly depend on the experimental conditions such as the temperature of the nozzle and the timing between the pulsed nozzle and the laser pulse. The long-lifetime component in Fig. 12 is assigned to the signals originating from the higher clusters larger than the dimer and/or the non-reactive $7AI_2$ dimer. The two time profiles due to $7AI_2$ are well reproduced with single exponential decays. The best-fitted time constants for the zero-point level and the 1σ state obtained from Figs. 12a and 12b are 1.9 ± 0.9 ps and 860 ± 300 fs, respectively. The decay time of the intermolecular stretching vibration is about a half that of the zero-point level. This result clearly shows the promoting character of the intermolecular stretching vibration.

We carefully measured the FE spectrum of $7AI_2$ with the nanosecond laser pulse, and obtained a bandwidth of the origin band to be 2.7 cm^{-1}, providing a time constant of $\tau_{0-0} \approx 2$ ps.[44]

However, the time constants of $\tau \approx 650$–660 fs, which were obtained by femtosecond experiments[37,39–41] for the nearly no excess energy in the S_1 state, were ascribed to single-proton transfer from the normal form to the intermediate state. The time constants obtained from the femtosecond experiments are contradictory to the bandwidth of the origin band in the FE spectrum, because it should be much broader than 2.7 cm^{-1} if single-proton transfer really occurs on a time scale of 650–660 fs. In contrast, the time constant (1.9 ± 0.9 ps) obtained by picosecond experiment is in good agreement with the bandwidth of the origin band. The time constants of $\tau \approx$ 650–660 fs obtained from the femtosecond experiments in the gas phase[37,39–41] agree with $\tau = 860 \pm 300$ fs within the experimental errors, which corresponds to the decay of the 1σ state from the picosecond experiment. Thus, the comparison of the data from the femtosecond and those from the picosecond experiments indicates that the bi-exponential decay profiles obtained by the femtosecond experiments at $\Delta E = 0$ kcal[37] are due to simultaneous excitation of the origin and the 1σ state with different lifetimes. It should be noted that the relative intensity of the short component with $\tau \approx 650$ fs in Ref. 37 was very weak when the excess energy was nearly zero. We infer that the origin band was dominantly excited by the femtosecond laser pulse when the frequency of the laser was tuned to the origin, but the 1σ state might be weakly excited by the blue-edge region of the laser profile in the femtosecond REMPI experiment, providing the bi-exponential decay profile.

The decay profiles of $7AI_2$ fitted to the single exponential functions observed in our study suggest that no stable intermediate state exists in the ESDPT reaction. This result is consistent with the concerted mechanism of the ESDPT reaction. The measurement of the UV–UV hole-burning spectra of the $7AI_2$ isotopomers suggested that femtosecond pulse with a width of $\approx$150 fs could not excite the single vibronic state.[37] The observed single exponential decays with picosecond laser are consistent with our suggestion from UV–UV hole-burning spectra. Our results unambiguously preclude the bi-exponential decays from the single vibronic state reported by Douhal et al.[37]

The origin of the discrepancies between our experiment and that of Castleman's group[39–41] is not clear. The femtosecond laser used for the Coulomb explosion experiment could not separately excite the single vibronic state. A question raised by Catalán et al. is that the single-proton transfer may occur from the ionized state to an ionic intermediate stable minimum before the Coulomb explosion on the basis of ab-initio calculations of the potential energy curve for the ionic state.[51,53] Recent calculations by Chen and Chao[59] also suggested the possibility of occurrence of single-proton transfer from the ionic state of the normal dimer to an intermediate minimum. Experimental studies on the potential of the $7AI_2$ ion will be performed to examine the calculated potentials.

7. DF Spectra and KIE

7.1 DF Spectra of $7AI_2$ and Isotopomers. The DF spectra of $7AI_2$ in solution or in matrix were measured by several group.[18–23] Very recently, Catalán et al.[29] reported that no tautomer emission was observed in the DF spectra of $7AI_2$-*dd* in a low-temperature matrix, Fuke et al.[36] observed only the tautomer fluorescence in the DF spectrum of $7AI_2$ measured by exciting the origin band of jet-cooled $7AI_2$-*hh*. We observed the DF spectra of $7AI_2$-*hd* and $7AI_2$-*dd* as well as those of $7AI_2$-*hh* to investigate the KIE on ESDPT.

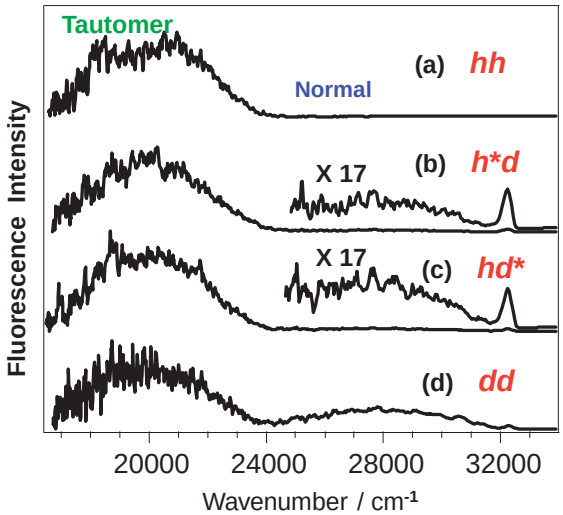

Fig. 13. DF spectra of $7AI_2$-*hh*, $7AI_2$-*h*d*, $7AI_2$-*hd**, and $7AI_2$-*dd* measured by exciting the 0–0 transitions of each dimer. The relative photon number is indicated as the intensity of fluorescence. This figure was made based on Ref. 44.

In the DF spectra in Fig. 13, the intensities are converted to relative photon numbers. The DF spectra of four isotopomers are observed following the excitation of the origin bands. In Fig. 13a, fluorescence from the tautomer of $7AI_2$-*hh* is observed in the visible region, whereas fluorescence from the normal dimer in the UV region is absent. This result is consistent with the occurrence of rapid ESDPT reaction ($\tau_{PT} = 1.9$ ps) and a very low fluorescence quantum yield (2.9×10^{-5}) for the normal dimer of $7AI_2$-*hh* measured in the condensed phase.[30–32] Figures 13b and 13c show the DF spectra of $7AI_2$-*h*d* and $7AI_2$-*hd**, respectively. In these spectra, weak UV fluorescence from the normal dimer is detected, together with the largely Stokes-shifted tautomer fluorescence. The observation of the normal dimer fluorescence from $7AI_2$-*h*d* and $7AI_2$-*hd** indicate that the excited-state proton/deuteron transfer (ESPDT) rates for $7AI_2$-*h*d* and $7AI_2$-*hd** are slower than the ESDPT rate for $7AI_2$-*hh*. The relative intensity ratios of the normal dimer fluorescence to the tautomer fluorescence are different for $7AI_2$-*h*d* and for $7AI_2$-*hd**; the normal dimer fluorescence is more strongly observed in $7AI_2$-*hd** than in $7AI_2$-*h*d*. Figure 13d shows the DF spectrum of $7AI_2$-*dd*. In this spectrum, the normal dimer fluorescence is clearly observed, together with the tautomer fluorescence. The strongly observed normal dimer fluorescence of $7AI_2$-*dd* indicates that the excited-state double-deuteron transfer (ESDDT) rate for $7AI_2$-*dd* is much slower than the ESPDT rates for $7AI_2$-*hd** and $7AI_2$-*h*d*. The reductions in the ESPDT and ESDDT rates for the deuterated $7AI_2$ dimers as compared with the ESDPT rate for the undeuterated $7AI_2$ dimer suggest that the ESDPT reaction of $7AI_2$ proceeds through the tunneling mechanism in the gas phase.

Figure 14 shows the DF spectra of $7AI_2$-*dd* measured by exciting the 0–0 band, 1β, and 1σ. The ratio of the tautomer

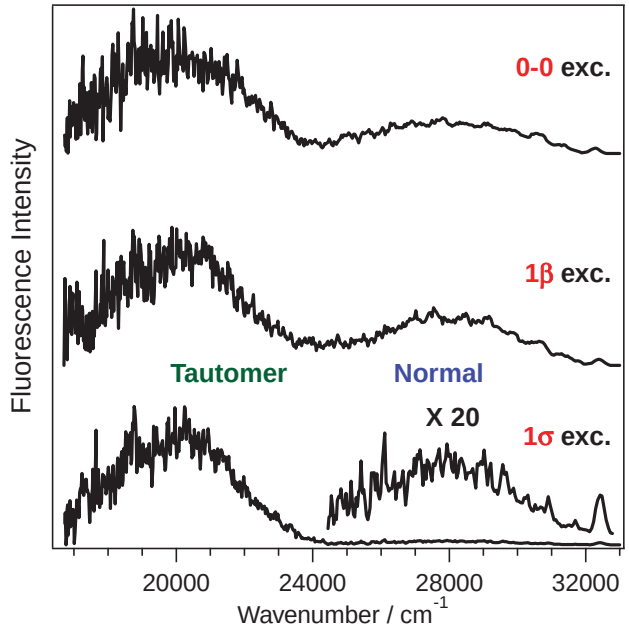

Fig. 14. DF spectra of $7AI_2$-*dd* measured by exciting the transitions to the zero-point level and intermolecular vibrations 1σ and 1β. The relative photon number is indicated as the intensity of fluorescence. This figure was made based on Ref. 44.

fluorescence to the normal fluorescence remarkably decreases for the excitation of the 1σ state as compared with the ratio for the 0–0 excitation. This observation is consistent with the promoting nature of the σ mode in ESDPT. However, the excitation of 1β slightly increases the ratio. Thus, the 1β mode has a suppressing nature, but its effect on the ESDPT rate is not so large.

7.2 Mechanism of ESDPT Revealed by KIE. The ESPDT and ESDDT rate constants for the deuterated $7AI_2$ dimers can be estimated from the relative intensity ratios of the normal dimer fluorescence to the tautomer fluorescence by considering a kinetic model schematically represented in Fig. 15. The relative fluorescence intensity in Fig. 13 is converted to the relative photon numbers, therefore, the intensity ratio of the normal dimer fluorescence to the tautomer fluorescence corresponds to the relative ratio of the fluorescence quantum yields of the normal dimers (Φ^n) to the products of the quantum yield of the ESPDT or ESDDT reaction and the fluorescence quantum yield of the tautomers (Φ^t).

$$\frac{I(\text{Normal})}{I(\text{Tautomer})} = \frac{\Phi^n}{\Phi^t}, \tag{4}$$

where I (Normal) and I (Tautomer) are the fluorescence intensities of the normal dimer and the tautomer, respectively. k_{PT} values are estimated with the Φ^n and Φ^t values in Eq. 5

$$k_{PT}^{XX} = \frac{k_r^n \cdot (k_r^t + k_{nr}^t)}{k_r^t \cdot \left(\frac{\Phi^n}{\Phi^t}\right)}, \tag{5}$$

where $k_r^{n(t)}$ and $k_{nr}^{n(t)}$ are the rate constants for the radiative (r) and nonradiative (nr) decay in the normal dimer (n) and the tautomer (t), respectively. Combining the reported radiative

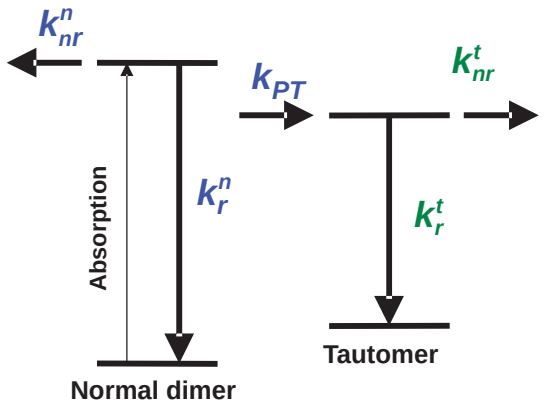

Fig. 15. Energy level diagram for the normal dimer and the tautomer of $7AI_2$. $k_r^{n(t)}$ and $k_{nr}^{n(t)}$ are the rate constants for the radiative and the nonradiative decay of the normal dimer (n) and the tautomer (t), respectively, and k_{PT} denotes the ESDPT rate constant. This figure was made based on Ref. 44.

Table 3. Relative Intensity Ratios of Normal Dimer to Tautomer and Rates for ESDPT, Proton/Deuteron Transfer, and Double-Deuteron Transfer in $7AI_2$-*hh* and Isotopomers[a)]

Species	I(Normal)/I(Tautomer)	k_{PT}/s^{-1}
$7AI_2$-*hh*	≈0	$(5.3 \pm 1.1) \times 10^{11}$ [b)]
$7AI_2$-*h*d*	0.029 ± 0.002	$(9.8 \pm 0.6) \times 10^9$
$7AI_2$-*hd**	0.042 ± 0.006	$(6.9 \pm 1.1) \times 10^9$
$7AI_2$-*dd*	0.36 ± 0.05	$(7.0 \pm 1.0) \times 10^8$

a) Ref. 44. b) Obtained from a time constant of 1.9 ps in Ref. 45.

and nonradiative lifetimes of the normal dimer and the tautomer[30–32] with the decay times obtained from picosecond measurement,[45] we obtained the rate constants k_{PT}^{XX}, which are distinguished with notations k_{PT}^{hh}, k_{PT}^{hd}, and k_{PT}^{dd} for ESDPT, ESPDT, and ESDDT, respectively. The fluorescence intensity ratios and the rate constants are summarized in Table 3.

It should be noted that the ESDDT rate constant k_{PT}^{dd} exhibits a prominent KIE (Table 3). However, the corresponding value measured in the condensed phase at room temperature is very different from the present result; the ratio k_{PT}^{hh}/k_{PT}^{dd} (= 1.5–5)[20,30–33] is much smaller than the corresponding value of 760 obtained in this study. We infer that the population in the excited states involving the intermolecular stretching mode predominantly contributes to the decay profiles observed in the condensed phase.

The dual fluorescence from $7AI_2$-h^*d and $7AI_2$-hd^* provides insights into the mechanism of ESDPT. The following schemes are assumed for the stepwise mechanism and the concerted mechanism,

$$\text{Normal dimer} \xrightarrow{k_1} \text{Intermediate} \xrightarrow{k_2} \text{Tautomer}, \tag{6}$$

$$\text{Normal dimer} \xrightarrow{k} \text{Tautomer}, \tag{7}$$

where k_1 and k_2 indicate the single-proton (or deuteron) transfer rate constants,[37,39–41] while k is the double-proton transfer rate constant.[30–32] A stable intermediate state should exist in

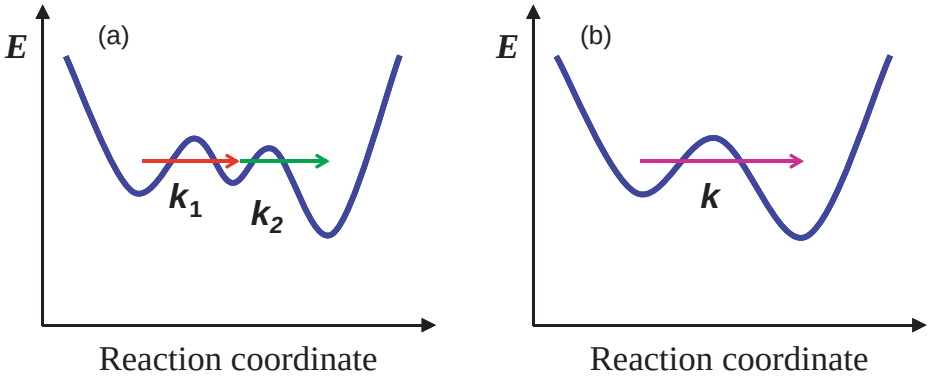

Fig. 16. Model potential curves for ESDPT along the reaction coordinate. A potential minimum exists between the two potential minima corresponding to the normal dimer and the tautomer in (a), where two single-proton transfer rates are indicated with k_1 and k_2. No potential minimum exists between the two minima in (b), where ESDPT rate is indicated with k.

the stepwise mechanism as illustrated in Fig. 16a. In this scheme, k_1 may exhibit very large KIE in $7AI_2$-hd^*, because the excitation is localized in the 7AI-d moiety, so that the single-deuteron transfer should occur before the single-proton transfer. In contrast, k_2 should show a large KIE in $7AI_2$-h^*d. Therefore, the intensity ratio of the normal dimer fluorescence to the tautomer fluorescence of $7AI_2$-hd^* must be much larger than that of $7AI_2$-h^*d, because the single-proton/deuteron transfer must occur through tunneling. The tunneling reaction generally show a prominent H/D isotope effect. However, the ratio I(Normal)/I(Tautomer) for $7AI_2$-h^*d is only 1.4 times larger than that for $7AI_2$-hd^*. This implies that the excited-state potential along the reaction coordinate has no intermediate minimum as shown in Fig. 16b, and that the ESDPT reaction occurs via the concerted mechanism as indicated in Fig. 16b. The argument from KIE is consistent with the picosecond REMPI experiment.

The mechanism of ESDPT in $7AI_2$ could be compared with that in the 1-azacarbazole dimer ($1AC_2$) studied by Fuke et al. with electronic spectroscopy and picosecond time-resolved fluorescence spectroscopy in a supersonic free jet expansion.[77,78] The bandwidths in the FE spectrum of $1AC_2$ are much narrower than those of $7AI_2$, suggesting that the ESDPT rate is much slower in $1AC_2$.[77] The decay profiles obtained by the excitation of the origin and intermolecular vibrations were fitted to single exponential functions.[78] The time constants were determined to be 330, 130, and 355 ps for the excitation of the origin, $0^0 + 109$ and $0^0 + 67\,cm^{-1}$ vibrations, respectively, where the $0^0 + 109$ and $0^0 + 67\,cm^{-1}$ vibrations were assigned to the intermolecular stretching and intermolecular bending fundamentals. The observation of single exponential decays is consistent with the concerted mechanism. No evidence of the existence of the reaction intermediate state in ESDPT has been reported for $1AC_2$.

8. New Paradigm of ESDPT in $7AI_2$

By comparing the k_{PT} values for the three $7AI_2$ dimers in Table 3, we have found large kinetic isotope effects on the ESDPT rate: $k_{PT}^{hh}/k_{PT}^{hd} \approx 63$, $k_{PT}^{hd}/k_{PT}^{dd} \approx 12$, and $k_{PT}^{hh}/k_{PT}^{dd} \approx 760$, where k_{PT}^{hd} is approximated by $(k_{PT}^{h^*d} + k_{PT}^{hd^*})/2$. The prominent KIE suggests that the first deuterium substitution strongly influences the reaction rate, as compared with the second deuterium substitution, i.e. a prominent *asymmetric kinetic isotope effect* is found. It should be noted that k_{PT}^{dd} is nearly three orders smaller than k_{PT}^{hh}. We infer that an electronic reorganization occurs along with the proton or deuteron motions. The changes in the electron densities in the proton and deuteron acceptor sites may play an important role in the proton- and deuteron-transfer dynamics. In the case of $7AI_2$-hd, the change in the electron density in the proton acceptor site must be slow, because the deuteron transfer is much slower than the proton transfer. The motions of two transferring protons (or deuterons) may couple with each other through the electronic reorganization. In other words, there is a correlation between the two single-proton (or deuteron) transfer reactions, i.e., the ESDPT reaction of $7AI_2$ has a "*cooperative*" nature. We refer to the coupling of the proton motion and the reorganization of electrons in the ESDPT and ESDDT reactions as a "*dynamic cooperative effect*," which is different from the conventional cooperative nature of the hydrogen bond.[79] In the latter case, no proton or hydrogen transfer occurs and it represents a "*static cooperative effect*."

Very recently, we estimated the exciton splitting in the zero-point level of the lowest excited state of $7AI_2$-hh and $7AI_2$-dd to be $2.4\,cm^{-1}$. This value allows us to estimate the rate of the exciton transfer (ET) between the two monomer units to be about 3 ps when the occurrence of coherent ET is assumed. The ESDPT and ESDDT time constants for $7AI_2$-hh and $7AI_2$-dd are estimated to be 2 ps and 1 ns, respectively. Thus, the time scale of ESDPT is very similar to that of ET from one monomer unit to the other one, whereas the ESDDT time scale is much slower than the ET time scale. If the switching of exciton between the two monomer units occurs during ESDDT, the excited monomer unit in $7AI_2$-dd also quickly switches during the reaction. Therefore, the reaction dynamics of ESDPT and ESDDT may be very different due to the influence of ET in ESDPT and ESDDT. The coupling of two quantum effects, the exciton resonance interaction and double-proton transfer by tunneling, has not been reported.

9. Conclusion

We have investigated the mechanism of the ESDPT reaction in $7AI_2$ by using vibronic-state selective spectroscopy in the frequency and time domains. The results obtained from our

work are summarized as follows. (1) The lowest-excited state of the normal dimer of $7AI_2$, which is the initial state of ESDPT, should be classified into the weak coupling case of the exciton theory. Therefore, the symmetry of the excited-state dimer does not belong to the C_{2h} symmetry. (2) The femtosecond laser (fwhm $\approx$150 fs) may excite more than two vibronic states of $7AI_2$ in the S_1–S_0 region, which must be the origin of the bi-exponential decay profiles observed by Douhal et al. in the femtosecond transients.[37] In contrast, the picosecond laser used in our experiment can separately excite the single vibronic state, and each decay profile is fitted to a single exponential function, precluding the stepwise mechanism. (3) A prominent KIE has been observed in the ESDPT reaction in $7AI_2$. The reaction rate for $7AI_2$-*dd* is about 1/760 of that for $7AI_2$-*hh*. We suggested the occurrence of a *dynamic cooperative effect* in $7AI_2$ from the nonlinear KIE. (4) The small difference in the reaction rates between 7AI-h^*d and $7AI_2$-hd^* is consistent with the concerted mechanism.

The mechanism of ESDPT had been a matter of controversy for many years. We believe that final resolution of the stepwise versus concerted mechanism has been provided by our studies. We have suggested that the excited-state dynamics of $7AI_2$ is complicated due to the presence of two quantum effects, exciton resonance interaction and proton tunneling. In addition, the cooperative ESDPT reaction has not been well understood. Further experimental and theoretical studies on $7AI_2$ and similar double hydrogen-bonded dimers will provide a detailed picture of the excited-state dynamics, which is important to understand the mechanism of more complicated multi-proton-transfer reactions in various systems.

The authors thank Prof. N. Nishi and Dr. C. Okabe for their collaboration with the picosecond time-resolved study at Institute for Molecular Science. We thank Dr. N. Kanamaru (Nagoya University), Prof. K. Ohashi, Mr. A. Hara, and Mr. Y. Komoto (Kyushu University) for helpful discussions. This work was supported in part by Grant-in-Aid for Scientific Research No. 15250015 from the Japanese Ministry of Education, Culture, Sports, Science and Technology, and the "Nanotechnology Support Project" of the MEXT, Japan.

References

1 M. L. Bender, *Mechanism of Homogeneous Catalysis from Proteins to Proteins*, John & Wiley and Sons, New York, **1971**.
2 R. P. Bell, *The Tunneling Effect in Chemistry*, Chapman and Hall, New York, **1980**.
3 Special issue on Photoinduced Proton Transfer in Chemistry, Biology, and Physics, *J. Phys. Chem.* **1991**, *95*.
4 *Proton Transfer in Hydrogen-Bonded Systems*, ed. by T. Buntis, Plenum Press, New York and London, **1992**.
5 A. Douhal, F. Lahmani, A. H. Zewail, *Chem. Phys.* **1996**, *207*, 477.
6 *Atom Tunneling Phenomena in Physics, Chemistry, and Biology*, ed. by T. Miyazaki, Springer, Berlin, **2004**.
7 T. Carrington, W. H. Miller, *J. Chem. Phys.* **1986**, *84*, 4364.
8 W. Siebrand, Z. Smedarchina, M. Z. Zgierski, A. Fernándes-Ramos, *Int. Rev. Phys. Chem.* **1999**, *18*, 5.
9 H. Sekiya, Y. Nagashima, Y. Nishimura, *J. Chem. Phys.* **1990**, *92*, 5761.
10 K. Nishi, H. Sekiya, H. Kawakami, A. Mori, Y. Nishimura, *J. Chem. Phys.* **1999**, *111*, 3961.
11 R. R. Sadeghi, H. P. Cheng, *J. Chem. Phys.* **1999**, *111*, 2086.
12 R. Pomes, B. Roux, *Biophys. J.* **1996**, *71*, 19.
13 Y. Matsumoto, T. Ebata, N. Mikami, *J. Phys. Chem. A* **2002**, *106*, 5591.
14 Z. Smedarchina, W. Siebrand, A. Fernández-Ramos, Q. Cui, *J. Am. Chem. Soc.* **2003**, *125*, 243.
15 C. Tanner, C. Manca, S. Leutweyler, *Science* **2003**, *302*, 1736.
16 J. D. Watson, F. H. C. Crick, *Nature* **1953**, *171*, 737.
17 P.-O. Löwdin, *Rev. Mol. Phys.* **1963**, *35*, 724.
18 C. A. Taylor, M. A. El-Bayoumi, M. Kasha, *Proc. Natl. Acad. Sci. U.S.A.* **1969**, *63*, 253.
19 K. C. Ingham, M. Abu-Elgheit, M. A. El-Bayoumi, *J. Am. Chem. Soc.* **1971**, *93*, 5023.
20 K. C. Ingham, M. A. El-Bayoumi, *J. Am. Chem. Soc.* **1974**, *96*, 1674.
21 W. M. Hetherrington, III, R. H. Micheels, K. B. Eisenthal, *Chem. Phys. Lett.* **1979**, *66*, 230.
22 H. Bulska, A. Chodkowska, *J. Am. Chem. Soc.* **1980**, *102*, 3259.
23 H. Bulska, A. Grabowski, B. Pakula, J. Sepiol, J. Waluk, U. P. Wild, *J. Lumin.* **1984**, *29*, 65.
24 K. Tokumura, Y. Watanabe, M. Itoh, *Chem. Phys. Lett.* **1984**, *111*, 379.
25 K. Tokumura, Y. Watanabe, M. Udagawa, M. Itoh, *J. Am. Chem. Soc.* **1987**, *109*, 1346.
26 P. Share, M. Pereira, M. Sarisky, S. Repinec, R. M. Hochstrasser, *J. Lumin.* **1991**, *48/49*, 204.
27 Y. Chen, R. L. Rich, F. Gai, J. W. Petrich, *J. Phys. Chem.* **1993**, *97*, 1770.
28 J. Waluk, *Acc. Chem. Res.* **2003**, *36*, 832.
29 J. Catalán, P. Perez, J. C. del Valle, J. L. G. de Paz, M. Kasha, *Proc. Natl. Acad. Sci. U.S.A.* **2004**, *101*, 419.
30 S. Takeuchi, T. Tahara, *Chem. Phys. Lett.* **1997**, *277*, 340.
31 S. Takeuchi, T. Tahara, *J. Phys. Chem. A* **1998**, *102*, 7740.
32 S. Takeuchi, T. Tahara, *Chem. Phys. Lett.* **2001**, *347*, 108.
33 M. Chachisvilis, T. Fiebig, A. Douhal, A. H. Zewail, *J. Phys. Chem. A* **1998**, *102*, 669.
34 T. Fiebig, M. Chachisvilis, M. Manger, A. H. Zewail, A. Douhal, I. Garcia-Ochoa, A. de La Hoz Ayuso, *J. Phys. Chem. A* **1999**, *103*, 7419.
35 K. Fuke, H. Yoshiuchi, K. Kaya, *J. Phys. Chem.* **1984**, *88*, 5840.
36 K. Fuke, K. Kaya, *J. Phys. Chem.* **1989**, *93*, 614.
37 A. Douhal, S. K. Kim, A. H. Zewail, *Nature* **1995**, *378*, 260.
38 R. Lopez-Martens, P. Long, D. Solgadi, B. Soep, J. Syage, P. Millie, *Chem. Phys. Lett.* **1997**, *273*, 219.
39 D. E. Folmer, L. Poth, E. S. Wisniewski, A. W. Castleman, Jr., *Chem. Phys. Lett.* **1998**, *287*, 1.
40 D. E. Folmer, E. S. Wisniewski, A. W. Castleman, Jr., *Chem. Phys. Lett.* **2000**, *318*, 637.
41 D. E. Folmer, E. S. Wisniewski, S. M. Hurley, A. W. Castleman, Jr., *Proc. Natl. Acad. Sci. U.S.A.* **1999**, *96*, 12980.
42 K. Sakota, A. Hara, H. Sekiya, *Phys. Chem. Chem. Phys.* **2004**, *6*, 32.
43 K. Sakota, H. Sekiya, *J. Phys. Chem. A* **2005**, *109*, 2718.
44 K. Sakota, H. Sekiya, *J. Phys. Chem. A* **2005**, *109*, 2722.

45 K. Sakota, C. Okabe, N. Nishi, H. Sekiya, *J. Phys. Chem. A* **2005**, *109*, 5245.
46 A. Nakajima, M. Hirano, R. Hasumi, K. Kaya, H. Watanabe, C. C. Carter, J. M. Williamson, T. A. Miller, *J. Phys. Chem. A* **1997**, *101*, 392.
47 H. Yokoyama, H. Watanabe, T. Omi, S. Ishiuchi, M. Fujii, *J. Phys. Chem. A* **2001**, *105*, 9366.
48 A. Douhal, M. Moreno, J. M. Lluch, *Chem. Phys. Lett.* **2000**, *324*, 75.
49 A. Douhal, M. Moreno, J. M. Lluch, *Chem. Phys. Lett.* **2000**, *324*, 81.
50 M. Moreno, A. Douhal, J. M. Lluch, *J. Phys. Chem. A* **2001**, *105*, 3887.
51 J. Catalán, J. C. del Valle, M. Kasha, *Proc. Natl. Acad. Sci. U.S.A.* **1999**, *96*, 8338.
52 J. Catalán, J. C. del Valle, M. Kasha, *Proc. Natl. Acad. Sci. U.S.A.* **2002**, *99*, 5799.
53 J. Catalán, J. C. del Valle, M. Kasha, *Chem. Phys. Lett.* **2000**, *318*, 629.
54 J. C. del Valle, M. Kasha, J. Catalán, *Int. J. Quantum Chem.* **2000**, *77*, 118.
55 L. Serrano-Andres, M. Merchan, A. C. Borin, J. Stalring, *Int. J. Quantum Chem.* **2001**, *84*, 181.
56 S. Mente, M. Maroncelli, *J. Phys. Chem. A* **1998**, *102*, 3860.
57 V. Guallar, V. S. Batista, W. H. Miller, *J. Chem. Phys.* **1999**, *110*, 9922.
58 J. R. Van Hise, *Mol. Phys.* **2001**, *99*, 1347.
59 H.-Y. Chen, I. Chao, *ChemPhysChem.* **2004**, *5*, 1855.
60 K. Iwahashi, N. Yamamoto, T. Fukuchi, J. Furusawa, H. Sekiya, *Chem. Phys.* **2001**, *270*, 333.
61 K. Nishi, H. Sekiya, T. Mochida, T. Sugawara, Y. Nishimura, *J. Chem. Phys.* **2000**, *112*, 5002.
62 K. Sakota, K. Nishi, K. Ohashi, H. Sekiya, *Chem. Phys. Lett.* **2000**, *322*, 407.
63 K. Nakabayashi, S. Kamo, H. Sakuragi, N. Nishi, *J. Phys. Chem. A* **2001**, *105*, 8605.
64 C. Okabe, K. Nakabayashi, N. Nishi, H. Sekiya, *J. Chem. Phys.* **2004**, *121*, 9436.
65 J. Frenkel, *Phys. Z. Sowjetunion* **1936**, *9*, 158.
66 R. L. Fulton, M. Gouterman, *J. Chem. Phys.* **1961**, *35*, 1059.
67 R. L. Fulton, M. Gouterman, *J. Chem. Phys.* **1964**, *41*, 2280.
68 E. G. McRae, W. Siebrand, *J. Chem. Phys.* **1964**, *41*, 905.
69 T. Förster, *Delocalization Excitation and Excitation Transfer*, in *Modern Quantum Chemistry*, ed. by O. Sinanoglu, Academic Press, New York, **1965**, Vol. III.
70 N. Kanamaru, *J. Mol. Spectrosc.* **2004**, *225*, 55.
71 A. Hara, Y. Komoto, K. Sakota, R. Miyoshi, Y. Inokuchi, K. Ohashi, K. Kubo, E. Yamamoto, A. Mori, N. Nishi, H. Sekiya, *J. Phys. Chem. A* **2004**, *108*, 10789.
72 Y. Komoto, K. Sakota, H. Sekiya, *Chem. Phys. Lett.* **2005**, *406*, 15.
73 A. Held, D. W. Pratt, *J. Am. Chem. Soc.* **1990**, *112*, 8629.
74 A. Held, D. W. Pratt, *J. Chem. Phys.* **1992**, *96*, 4869.
75 A. Muller, F. Talbot, S. Leutwyler, *J. Chem. Phys.* **2002**, *116*, 2836.
76 C. A. Southern, D. H. Levy, J. A. Stearns, G. M. Florio, A. Longarte, T. S. Zwier, *J. Phys. Chem. A* **2004**, *108*, 4599.
77 K. Fuke, T. Yabe, N. Chiba, T. Kohida, K. Kaya, *J. Phys. Chem.* **1986**, *90*, 2309.
78 K. Fuke, K. Tsukamoto, F. Misaizu, K. Kaya, *J. Chem. Phys.* **1991**, *95*, 4074.
79 O. Mó, M. Yáñez, J. E. Del Bene, I. Alkorta, J. Elguero, *ChemPhysChem.* **2005**, *6*, 1411, and references therein.

Hiroshi Sekiya was born in 1950 in Niigata, Japan. He graduated from Kanazawa University in 1973 and obtained his M.Sc. degree in 1975 from Kanazawa University. He graduated from Kyushu University and obtained Dr.Sc. degree in 1979. He became a Research Associate of the Research Institute of Industrial Science, Kyushu University in 1982. He studied the reaction dynamics of excited-state atoms and radicals and proton tunneling in polyatomic molecules under the supervision of Prof. Yukio Nishimura. He worked with Dr. Klaus Müller-Dethlefs in Technical University of Munich from 1991 to 1992 as a Humboldt Foundation Fellow. In 1995, he was appointed as an Associate Professor of the Faculty of Science, Kyushu University, under the supervision of Prof. Nobuyuki Nishi. In 1997, he was appointed as a Full Professor of the Faculty of Science, Kyushu University. His recent research interests are intermolecular interactions and excited-state dynamics of molecular clusters involving quantum effects such as tunneling, exciton resonance interaction, and nonadiabatic transitions.

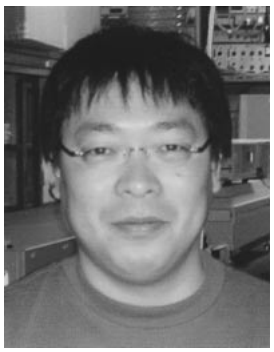

Kenji Sakota was born in 1976 in Yamaguchi, Japan. He graduated from Kyushu University in 1999 and obtained his M.Sc. degree in 2001 from Kyushu University. He entered the Dr.Sc. course in 2001 and awarded JSPS Research Fellowships for Young Scientists from 2001 to 2002. He became a Research Associate of the Faculty of Sciences, Kyushu University in 2002 under the supervision of Prof. Hiroshi Sekiya. He obtained a Dr.Sc. degree from Kyushu University in 2005. His interests are reaction dynamics of hydrogen-bonded clusters such as proton transfer, exciton transfer, and structural isomerization.